Available online at www.sciencedirect.com
SCIENCE DIRECT®
International Journal of Heat and Mass Transfer 47 (2004) 1313–1323
International Journal of HEAT and MASS TRANSFER
www.elsevier.com/locate/ijhmt

Investigation of influence of thermal accommodation on oscillating micro-flow

Jae Hyun Park [1], Seung Wook Baek *

Division of Aerospace Engineering, Department of Mechanical Engineering, Korea Advanced Institute of Science and Technology, 373-1 Kusung-dong, Yusung-ku, Taejon 305-701, South Korea

Received 18 October 2002; received in revised form 16 August 2003

Abstract

Thermal accommodation coefficient, one of the fundamental parameters in rarefied gas dynamics, is usually introduced to account for the fraction of incident molecules interacting with solid surface in a diffusive manner. In the present study, the effects of thermal accommodation on the unsteady one-dimensional micro-flow are examined, when the oscillating flow input are applied, by employing the unsteady DSMC technique. Since the temperature jump relation has been usually accepted as the thermal boundary condition in the analysis of MEMS flow, it is also focused on in this study. To this end, the wall heat fluxes are also obtained indirectly by applying the temperature jump relation to DSMC temperature profiles. For the case of small system with full thermal accommodation, the indirect wall heat fluxes calculated using the DSMC and free molecular approximation are almost exactly overlapped whereas two direct results show an obvious deviation, because the propagation speed of heat is different. A variation in the thermal accommodation coefficient is observed to only affect the wall properties such as heat flux and wall pressure rather than flow properties. In addition, the difference between indirect and direct heat flux remained being unchanged even if the thermal accommodation coefficient is varied. These aspects need to be kept in mind when analyzing the problem with the temperature jump boundary condition.

Keywords: MEMS; Unsteady micro-flow; Temperature jump; DSMC; Knudsen number; Acoustic reynolds number; Thermal accommodation coefficient

1. Introduction

In spite of the rapid development in the micro-fabrication technologies for MEMS devices, a fundamental understanding of fluid flow and heat transfer in micro-scale is still not satisfactory. Especially, a study of unsteady heat transfer in micro-flow is rarely found while most previous theoretical or numerical works regarding micro-systems have concentrated on the flow characteristics [1]. Practically, a detailed analysis of micro-flow with heat transfer would be very helpful in designing the efficient micro-space propulsion systems such as μ-arcjet and μ-resistojet [2].

Considering these points, Park et al. [3] investigated the unsteady micro-scale heat transfer by employing the unsteady DSMC technique. However, they assumed the diffuse wall therein. Different from the previous work, the present study concentrates on the effect of thermal accommodation on the unsteady micro-system.

Experiments about gas/surface interaction at normal temperature indicate that the reflection process can be successfully modeled as a diffuse reflection with complete thermal accommodation. This behavior may be a consequence of such surfaces as being microscopically

* Corresponding author. Tel.: +82-42-869-3714; fax: +82-42-869-3710.
E-mail addresses: jaepark@uiuc.edu (J.H. Park), swbaek@kaist.ac.kr (S.W. Baek).
[1] Present address: Beckman Institute for Advanced Science and Technology, University of Illinois at Urbana-Champaign, 405 North Mathews Avenue, Urbana, IL 61801, USA.

0017-9310/$ - see front matter © 2003 Elsevier Ltd. All rights reserved.
doi:10.1016/j.ijheatmasstransfer.2003.08.028

Nomenclature

c_0	speed of sound ($=\sqrt{\frac{\gamma k_B T}{m}}$)
c_{mp}	most probable speed ($=\sqrt{\frac{2k_B T}{m}}$)
E	energy
f	velocity distribution function
k_B	Boltzmann constant ($=1.38054\times10^{-23}$ J/K)
Kn	Knudsen number ($=\lambda/L$)
L	system size
m	molecular mass
Re	Reynolds number
q	heat flux
t	time
T	temperature
u	bulk velocity (x-direction)
γ	specific heat ratio
λ	mean free path
ρ	density
σ_T	thermal accommodation coefficient
ω	excitation frequency
ξ	thermal velocity (x-direction)
η	thermal velocity (y-direction)
ζ	thermal velocity (z-direction)

Subscripts

0	rest state
m	medium
w	wall

rough with the incident molecules suffering multiple scattering, or with the molecules being momentarily trapped or absorbed on the surface. Most analytical and numerical studies have assumed the diffuse reflection, and fortunately, this appears to be adequate for the many practical gas flows [4].

Actually, the assumption of full thermal accommodation is valid only if the characteristic time of molecular energy exchange, t_{mol}, is infinitesimally small compared with other characteristic time of the system, t_{sys}. However, such a simplification cannot be applied to the following problems such as the flow field around satellite [5], the ultra-fast heating of small substance by laser [6], the highly oscillating signal propagation through rarefied medium [7], etc., since in these problems, t_{sys} is comparable to t_{mol}. Particularly, in the rarefied binary mixtures in which the two components have very different molecular masses, the fast sound (the frequency level is larger than 10^8 Hz) is generated [8,9], which is one of interesting phenomena in rarefied flow.

Extended from the previous work [3], in this study the one-dimensional unsteady micro-flow caused by oscillating flow input is investigated with emphasis on the effect of thermal accommodation. Although Park et al. [3] have pointed out that the Smoluchowski's jump relation induces some inevitable error, this study focuses on the effect of thermal accommodation on the jump relation, since it is still widely used as a thermal boundary condition for diverse governing equations [10–13]. The six different cases are considered and discussed in the below by varying system size and medium density, i.e., the Knudsen number and the acoustic Reynolds number. As a numerical tool, the DSMC method, which is validated through comparison with free molecular solutions, is adopted.

2. Problem definition and unsteady DSMC method

As schematically shown in Fig. 1, a plannar system filled with monatomic argon gas is considered, which is

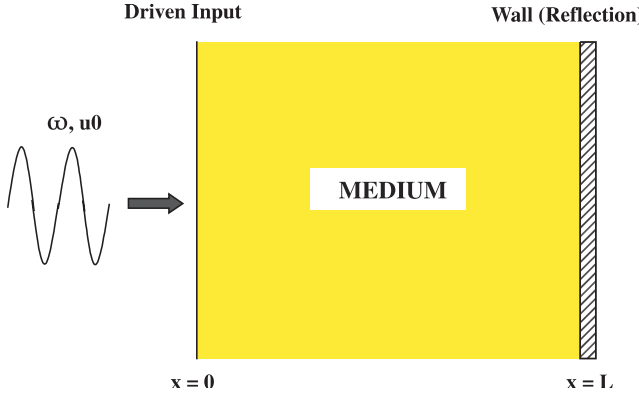

Fig. 1. Schematic of the problem.

similar to the previous study [3]. A fluctuating input is continuously excited at the left end by imposing a sinusoidal mean velocity oscillation of $u(t,x=0)=U(t)=U_0\sin(\omega t)$ where u is the mean velocity along x-direction, U_0 is the amplitude of excitation, ω is excitation frequency, and t is time. Then, it is introduced into the gas medium of length L initially at rest with $T_m = 300$ K. A solid wall with $T_w = 300$ K is located at the right end of the domain so that the impinging molecules are diffusely reflected there.

The unsteady DSMC code used in this study is modified from the Bird's DSMC1U [4] that adopts No Time Counter (NTC) scheme and Variable Hard Sphere (VHS) Model. The oscillating molecular influx at left end is introduced to the domain through the Maxwellian reservoir method. Its detailed procedure is described in previous works [3,7] and it is skipped here.

Throughout the computations in this study, it is always ensured that there are more than 100 particles per cell on average and each cell size is taken less than 0.1λ in order to obtain the satisfactory accuracy. Here, λ is the mean free path of the molecules in medium. According to Hadjiconstantinou and Garcia [7], the computing time step Δt in unsteady DSMC simulation should be taken to be significantly smaller than λ/c_{mp} in which c_{mp} is the most probable speed given by $\sqrt{\frac{2k_BT}{m}}$. Moreover, when treating the fluctuating medium like in the present situation, the time step used should also satisfy $\Delta t \ll 2\pi/\omega$ to guarantee the enough resolution for unsteady signals. In this study, the computing time step is set to be $\Delta t = 0.1(\lambda/c_{mp})$. For this case, even the biggest Δt becomes the value of 2.1130×10^{-10} s which is much less than $2\pi/\omega \approx 6.28\times10^{-8}$ s. The ensemble average is obtained performing over 5000 realizations of stochastic process within a given time interval.

3. Free molecular solutions

In this study, the free molecular solutions for small oscillating signal propagation are considered for the comparison with unsteady DSMC results. To this end, the one-dimensional BGK model equation is linearized first by decomposing the variables as follows [14,15]:

$$f = f_0(1+\phi), \tag{1}$$

$$\rho = \rho_0(1+\omega), \tag{2}$$

$$T = T_0(1+\tau), \tag{3}$$

$$q_w = q_{w,0}(1+\theta_w), \tag{4}$$

where f is the velocity distribution function, ρ is density, T is temperature, and q_w is wall heat flux. The subscript 0 represents the initial rest state while ϕ, ω, τ, and θ_w is the propagating fluctuation of the corresponding variable. Apparently, the velocity u is directly represented by the fluctuation itself because the medium is initially at rest. Then, following Sone's approaches [14,15], we can easily obtain the following expressions for fluctuating properties in free molecular regime:

$$\omega = \frac{2}{\sqrt{\pi}}\int_{x/t}^{\infty}\overline{U}\xi\exp(-\xi^2)\mathrm{d}\xi, \tag{5}$$

$$\tau = \frac{2}{3\sqrt{\pi}}\int_{x/t}^{\infty}\overline{U}(2\xi^3-\xi)\exp(-\xi^2)\mathrm{d}\xi, \tag{6}$$

$$\theta = \frac{1}{2\sqrt{\pi}}\int_{x/t}^{\infty}\overline{U}(\xi^2+\xi^4)\exp(-\xi^2)\mathrm{d}\xi, \tag{7}$$

where

$$\overline{U} = U\left(t-\frac{x}{\xi}\right). \tag{8}$$

In the present study, the numerical integration adopts the Simpson's method to obtain values of above equations at each time step.

4. Temperature jump relation

In rarefied gas dynamics, one of the major problems is to model the interaction of gas molecules with a solid surface. The parameter accounting for this phenomenon is the very accommodation coefficient that represents the tendency of gas to accommodate the wall state. In terms of energy, the accommodation coefficient can be defined by [16]:

$$\sigma_T = \frac{E_i - E_r}{E_i - E_w}, \tag{9}$$

where E_i denotes the energy flux of the incident molecular stream, E_r denotes the energy carried away by the reflected molecules, and E_w denotes the energy that is carried away by the reflected molecules when the temperature of reflected molecular stream is assumed to be the same as the wall temperature T_w. σ_T in Eq. (9) is usually called as "thermal accommodation coefficient" distinguished from "tangential momentum accommodation coefficient (TMAC)" σ_v based on momentum accommodation at surface [17]. Physically, there exist two extreme conditions for the molecular reflection at wall. The first one is the perfectly specular reflection, in which the molecules elastically collide with wall so that the molecular velocity component normal to the surface is reversed while that parallel to the surface remains unchanged. As a result, the impinging molecular stream exerts no shear stress on the surface except the normal direction to the wall. In this case, it becomes $E_i = E_r$ so that σ_T becomes zero. The other condition is the perfectly diffusive reflection, in which the incident molecules have their mean energy completely adjusted or

"accommodated" to the surface for which it becomes $E_r = E_w$ so that σ_T is equal to unity. Rearranging Eq. (9), then we obtain

$$E_r = \sigma_T E_w + (1 - \sigma_T) E_i. \tag{10}$$

According to Eq. (10), the thermal accommodation coefficient represents a fraction of molecules that experience diffusive reflection at the solid surface. As discussed above, σ_T has the value ranging from 0 to 1.0.

The Smolochowski's temperature jump relation can be derived by considering the kinetic approach on conductive energy balance between gas and solid surface. When the impinging molecular stream is assumed in equilibrium, the resultant formula is given by [17]:

$$T_g - T_w = \frac{2 - \sigma_T}{\sigma_T} \left[\frac{2(\gamma - 1)}{\gamma + 1} \right] \frac{1}{R_g \rho_g \sqrt{2 R_g T_\infty / \pi}} (q_n);$$

$$q_n = K \left(\frac{\partial T}{\partial n} \right)_w, \tag{11}$$

or

$$T_g - T_w = \frac{2 - \sigma_T}{\sigma_T} \left[\frac{2\gamma}{\gamma + 1} \right] \frac{Kn}{Pr} \left(\frac{\partial T}{\partial n} \right)_w, \tag{12}$$

where T_g is the gas temperature at wall due to temperature jump while T_w is the actual wall temperature. γ, R_g and T_∞ are the specific heat ratio, the gas constant, and the mean temperature at a region sufficiently far from the wall, while K and Pr are thermal conductivity and the Prandtl number. Physically, this represents the heat flux toward wall, q_n, which can be actually calculated using the temperature difference at wall, $T_g - T_w$. In other words, once the gas temperature profiles are obtained using the DSMC or the free molecular approximation, the indirect heat flux can be calculated using the above temperature jump relation.

However, since some fundamental inaccuracy resides in the Smolochowski's relation, improved models satisfying a detailed balance were proposed by Cercignani and Lampis [18] and Lord [19]. Park et al. [3] also pointed out that the Smolochowski's relation may not be very accurate in unsteady micro-scale heat transfer.

Nevertheless, due to its simplicity and reasonable accuracy, many researchers have widely utilized the conventional temperature jump relation as a boundary condition for the rarefaction effects in the analysis of rarefied flow [10–13]. Considering these points, much part of present study focuses on the effect of thermal accommodation on the temperature jump relation.

5. Results and discussion

Similar to the authors' previous work [3], the present study examines the six cases with different system size and density for the fixed excitation condition where $U_0 = 0.15 c_0$ and $\omega = 1.0 \times 10^8$ Hz. Here, c_0 is the speed of sound as defined by $\sqrt{\frac{\gamma k_B T}{m}}$. The detailed computing conditions are listed in Table 1. In Case A, B, and C, the medium density ρ_0 is varied for a fixed system size L while Case D, E, and F have different domain sizes for a fixed medium density.

Two parameters of the acoustic Reynolds number Re_a and the Knudsen number Kn_L are listed in the table to represent the acoustic feature and the rarefaction degree of the medium for each situation. The acoustic Reynolds number is defined as

$$Re_a = \frac{c_0^2 \rho_0}{\omega \mu_0}, \tag{13}$$

where the viscosity μ_0 is given by

$$\mu_0 = \frac{1}{2} \rho_0 \lambda \overline{C}_{rms} \tag{14}$$

with

$$\overline{C}_{rms} = \sqrt{(\xi^2 + \eta^2 + \zeta^2)} = \sqrt{\frac{3 k_B T}{m}}. \tag{15}$$

Since the excitation frequency remains constant throughout the calculation, the acoustic Reynolds number actually represents the medium density. Different from the sound wave propagation problem through rarefied infinite medium [20,21], the present domain is finite. That is why two system parameters of Re_a and Kn_L are simultaneously required in the identification of a system. For the infinite case, since both acoustic Reynolds number and Knudsen number have the same

Table 1
Computational conditions considered in the present study

Case	Re_a/γ	ρ_0 [kg/m^3]	L [μm]	λ [μm]	$t_c \times 10^9$ [s]	Kn_L
A	0.5	0.1149	0.8067(0.25l)	0.7840	2.4296	0.9718
B	1	0.2285	0.8067(0.25l)	0.3920	1.2148	0.4859
C	2	0.4460	0.8067(0.25l)	0.1960	0.6074	0.2430
D	0.5	0.1149	1.6134(0.50l)	0.7840	2.4296	0.4859
E	0.5	0.1149	3.2266(1.00l)	0.7840	2.4296	0.2430
F	0.5	0.1149	6.4535(2.00l)	0.7840	2.4296	0.1215

Argon gas, $\omega = 1.0 \times 10^8$ Hz ($l = 3.2268$ μm), $T_m = T_w = 300$ K.

characteristic length $L = c_0/\omega$, there exists a following relation between Kn_a and Re_a:

$$Re_a = \sqrt{\gamma \frac{4}{3}} \times \frac{1}{Kn_a}, \tag{16}$$

where the subscript 'a' in Knudsen number denotes 'acoustic'.

Before investigating the effect of thermal accommodation, it is necessary to validate the present DSMC program. To this end, the DSMC calculation is carried out for six cases with full thermal accommodation ($\sigma_T = 1.0$) and the resultant wall heat fluxes are compared with their free molecular solutions in Fig. 2 which presents a temporal variation of normalized heat flux fluctuation at wall. Since both the wall temperature T_w and medium mean temperature T_m have the same value of 300 K, the fluctuation actually represents the net wall heat flux itself. T_0 and x^* in the figure denote the period $2\pi/\omega$ and normalized coordinate x/L, respectively. In each graph there are four types of heat fluxes depending on the method used: (1) θ_w(DSMC; direct) directly computed using the DSMC only, (2) θ_w(DSMC; ΔT) indirectly computed using the DSMC temperature profiles by applying temperature jump relation of Eq. (12) and (9) θ_w(FM; direct), directly computed using the free molecular approximation, and (4) θ_w(FM; ΔT) indirectly computed using the free molecular temperature profiles. The classification of four wall heat fluxes is summarized in Table 2. Since the Park et al. [3] have already shown that the wall heat fluxes calculated from the original Smoluchowski's relation are not much different from their alternatives from its higher-order modifications higher-order modifications, the classical relation is still taken into account for computation of θ_w(DSMC; ΔT) and θ_w(FM; ΔT).

In general, θ_w(DSMC) and θ_w(FM) agree well for Case A, B, and C which are of relatively small physical size. On the other hand, they differ significantly with incresaing the domain length as shown in Fig. 2(d)–(f). Especially, a perfect coincidence is found between two indirect heat fluxes of θ_w(DSMC; ΔT) and θ_w(FM; ΔT). Such an agreement in Case A, B, and C proves that the present DSMC analysis is accurate enough to investigate the small signal propagation through micro-flow in MEMS. However, Fig. 2(a)–(c) show that some deviations between θ_w(DSMC; direct) and θ_w (FM; direct) are

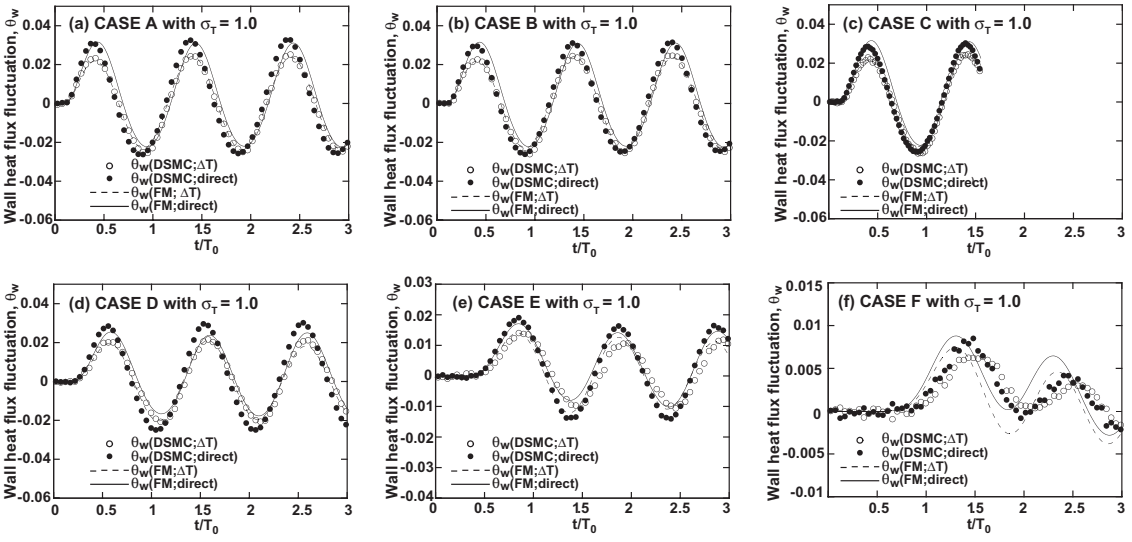

Fig. 2. Temporal variations of the normalized wall heat flux fluctuation using four different type of computations for various cases with $\sigma_T = 1.0$: (a) Case A; (b) Case B; (c) Case C; (d) Case D; (e) Case E; (f) Case F.

Table 2
Classification of wall heat fluxes

Method used for computation	How to obtain heat flux	
	Direct—θ_w(direct)	Indirect—$\theta_w(\Delta T)$ (temperature jump relation)
DSMC—θ_w(DSMC)	θ_w(DSMC; direct)	θ_w(DSMC; ΔT)
Free molecular approximation—θ_w(FM)	θ_w(FM; direct)	θ_w(FM; ΔT)

observed because the propagation speed of heat in the DSMC simulation is different from that in free molecular computation which does not involve the molecular collision. Contrary to heat flux, the propagation speed of temperature seems not to be varied depending on the degree of rarefaction, since θ_w(DSMC; ΔT) becomes exactly the same as θ_w(FM; ΔT). Tzou [6] already pointed out such temporal phase difference between heat and temperature propagation [6].

According to Park et al. [3], a deviation between direct θ_w(direct) and indirect $\theta_w(\Delta T)$ in either DSMC or free molecular computation, are due to the fundamental errors embedded in the Smoluchowski's temperature jump relation. As indicated in previous section, in the derivation of jump relation, it is assumed that the incident molecular flux is in equilibrium. It might be true in steady rarefied flow, however it may not be true in unsteady situation.

It becomes clearer when investigating it in the gas-kinetics viewpoint. Theoretically, the translational temperature and the heat flux toward wall are given as follows [3,4]:

$$T_{tr} = \overline{\sum_{cell} \frac{1}{2}\frac{m}{k_B}(\xi^2+\eta^2+\zeta^2)}, \tag{17}$$

$$q_w = \frac{N_p}{\Delta t N_{smp}}\left[\overline{\sum_{wall} m\frac{1}{2}(u^2+v^2+w^2)} + \overline{\sum_{wall} m\frac{1}{2}(\xi^2+\eta^2+\zeta^2)}\right](\because \bar{\xi}=\bar{\eta}=\bar{\zeta}=0), \tag{18}$$

where the 'cell' indicates the summation over all the molecules in the cell interested while the 'wall' denotes the statistical collection for both the incident and reflected molecules. The over-bar stands for 'ensemble average'. N_p is the number of molecules represented by every single simulated particle, Δt time step, and N_{smp} is the number of samples. A careful examination of Eqs. (17) and (18) reveals that the wall heat flux involves one more energy term of $\overline{\sum_{wall}\frac{1}{2}m(u^2+v^2+w^2)}$ which is attributed to mean velocities. The results in Fig. 2 assume a full thermal accommodation and furthermore, assume that the reflected molecular stream from right wall is always in complete equilibrium. Therefore, a degree of non-equilibrium at wall would result from a difference between incident and reflected molecular stream. As revealed in Fig. 3, more incident molecules are found at positive peak of heat flux rather than at negative peak of heat flux so that a more deviation arises between θ_w(direct) and $\theta_w(\Delta T)$ at positive peak of heat flux.

Now, we examine the effect of thermal accommodation on the flow properties such as density, temperature, and velocity. Figs. 4 and 5 compare their histories at an arbitrary selected position of $x^* = 0.75$ depending on σ_T for representative Case B and D, which have the same Kn_L of 0.4859. The results show that the effects of σ_T on the propagation speeds of density, velocity, and temperature are negligible. Although the other four cases investigated are not shown here, such a trend is still found therein. This is due to the system size chosen here with its mean free path. That is to say, the influence of thermal accommodation at right wall cannot fully prevail in the flow domain because the system size is so

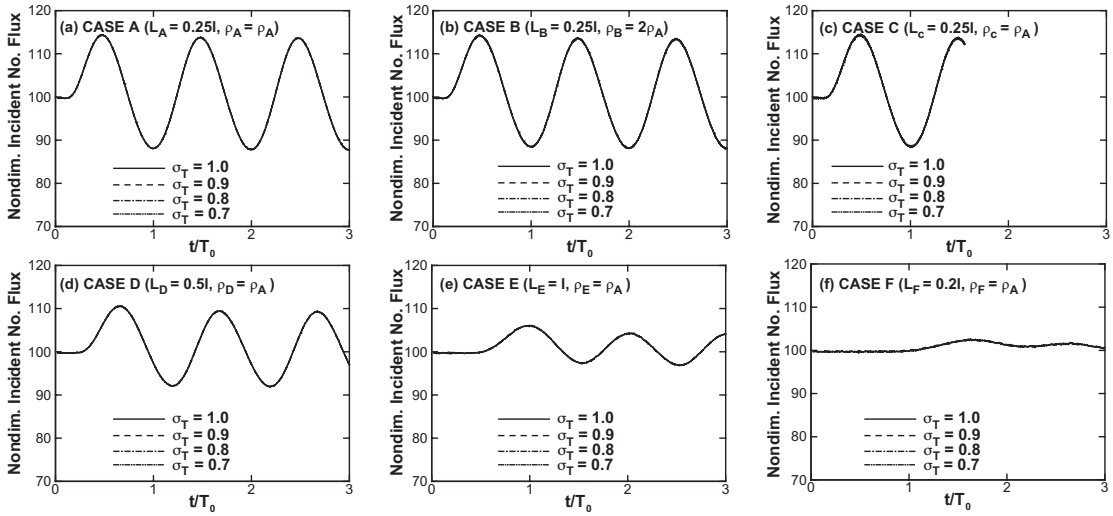

Fig. 3. Temporal variations of wall incident number flux depending on σ_T for various cases: (a) Case A; (b) Case B; (c) Case C; (d) Case D; (e) Case E; (f) Case F.

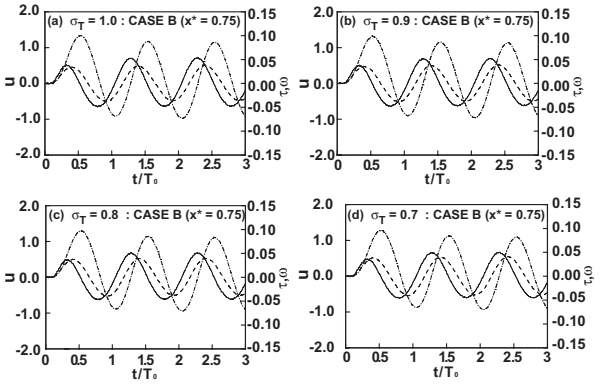

Fig. 4. Temporal variations of various flow properties at $x^* = 0.75$ for Case B with different σ_T: (a) $\sigma_T = 1.0$; (b) $\sigma_T = 0.9$; (c) $\sigma_T = 0.8$; (d) $\sigma_T = 0.7$ (—: velocity, - - - - -: temperature, – – – –: density).

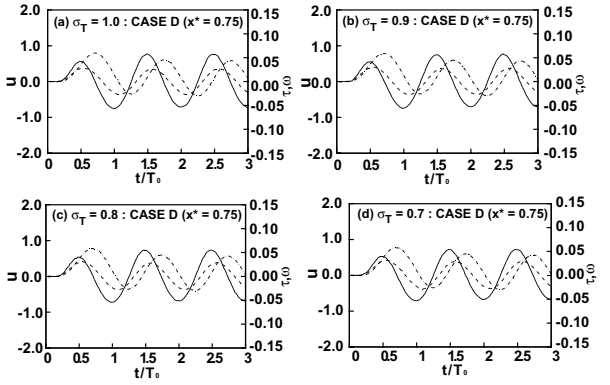

Fig. 5. Temporal variations of various flow properties at $x^* = 0.75$ for Case D with different σ_T: (a) $\sigma_T = 1.0$; (b) $\sigma_T = 0.9$; (c) $\sigma_T = 0.8$; (d) $\sigma_T = 0.7$ (—: velocity, - - - - -: temperature, – – – –: density).

small that the molecular collisions are not enough to fully transfer the external information at $x = 0$. As a result, the flow properties are mostly affected by the enforced excitation at left end. However, the effect by gas/surface interaction model would become remarkable in a larger system [2,22]. Also, Karniadakis and Beskok [17] shows that the temperature jump apparently appears in the Poiseuille flow through micro-channel, once the wall is not insulated, and that its magnitude increases as the flow Mach number increases.

Different from the flow properties, the wall properties such as heat flux and reflected pressure are severely affected by the variation of σ_T as shown in Figs. 6 and 7. Fig. 6 illustrates the temporal variations of wall heat flux depending on thermal accommodation coefficient for various cases. The averaged peak values in the figures are listed in Table 3. The heat fluxes represented by solid and dashed lines are obtained by applying the temperature jump relation to DSMC calculations. During a specular reflection process, the molecular velocity component normal to the surface is reversed while parallel one to the surface remain unchanged. A collection of molecules with such a process macroscopically results in the thermal insulation without net energy transfer onto wall. Hence, as the thermal accommodation coefficient decreases, the magnitude of net heat flux gradually decreases because the adiabatic portion of molecules increases. The reduction of wall heat flux is purely due to the change in molecular velocities. As presented in Fig. 3, the variation in σ_T does not incur a change in incident molecular number flux because it is rather affected by the enforced excitation than the wall condition. However, Fig. 7 shows that the reflected wall pressure is severely influenced by the change in σ_T, for the reflected

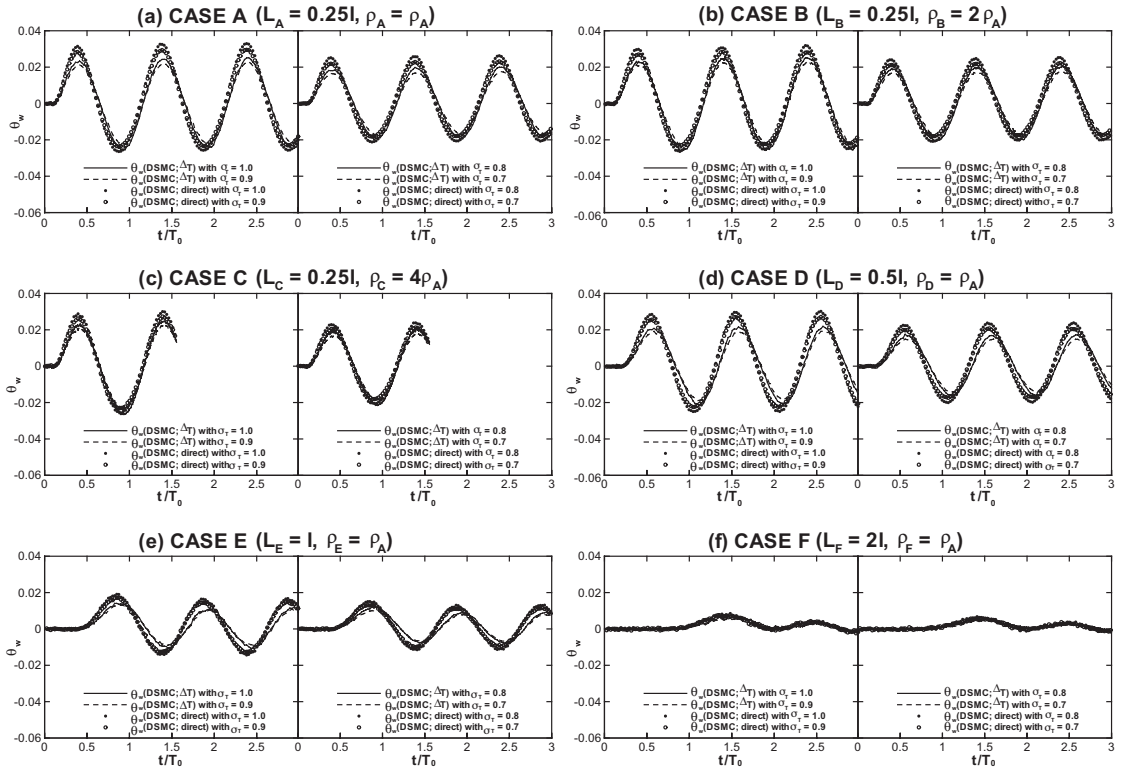

Fig. 6. Temporal variations of heat fluxes at wall directly and indirectly computed depending on σ_T for various cases: (a) Case A; (b) Case B; (c) Case C; (d) Case D; (e) Case E; (f) Case F.

molecular velocities are apparently varied depending on the degree of thermal accommodation. The wall pressure actually represents the averaged momentum difference between incoming and outgoing molecular streams. Different from the reflected wall pressure, the incident pressure remains almost unchanged, since the system behavior is mostly influenced by the enforced excitation at left end as discussed in Figs. 4 and 5. The inner medium pressure p is determined by the relation of $p = nk_B T_{trans}$ where n is number density and T_{trans} is the translational temperature. In this study dealing with monatomic argon gas, T_{trans} is equal to medium temperature T itself. Thus, it is quite clear that the medium pressure is not affected very much by the change in σ_T, considering the dynamic responses of temperature and density in Figs. 4 and 5.

Furthermore, in Fig. 8, a temporal variation of difference between θ_w(DSMC; direct) and θ_w(DSMC; ΔT) is plotted for six cases depending on σ_T. The figure shows that θ_w(DSMC; direct) – θ_w(DSMC; ΔT) is not so influenced by the gas/surface interaction model that the degree of error induced by the Smoluchowski's jump relation is neither reduced nor magnified depending on the surface condition. Such features should be always kept in mind when analyzing the problem with the temperature jump boundary condition.

6. Concluding remarks

A numerical study has been carried out to investigate the effect of thermal accommodation on the unsteady semi-confined one-dimensional micro-flow responding to the oscillating flow input. The unsteady DSMC technique was applied to the six cases with different system size and medium density. The thermal accommodation coefficient considered ranged from 0.7 to 1.0 with increment of 0.1. Since the temperature jump relation has been widely accepted as the thermal boundary condition in the analysis of MEMS flow, it was focused on in this study. For the case of small system with full thermal accommodation, a perfect overlap was observed between two indirect wall heat fluxes calculated the DSMC and free molecular approximation, whereas two direct results without using temperature jump relation yielded an obvious deviation, because the propagation speed of heat is

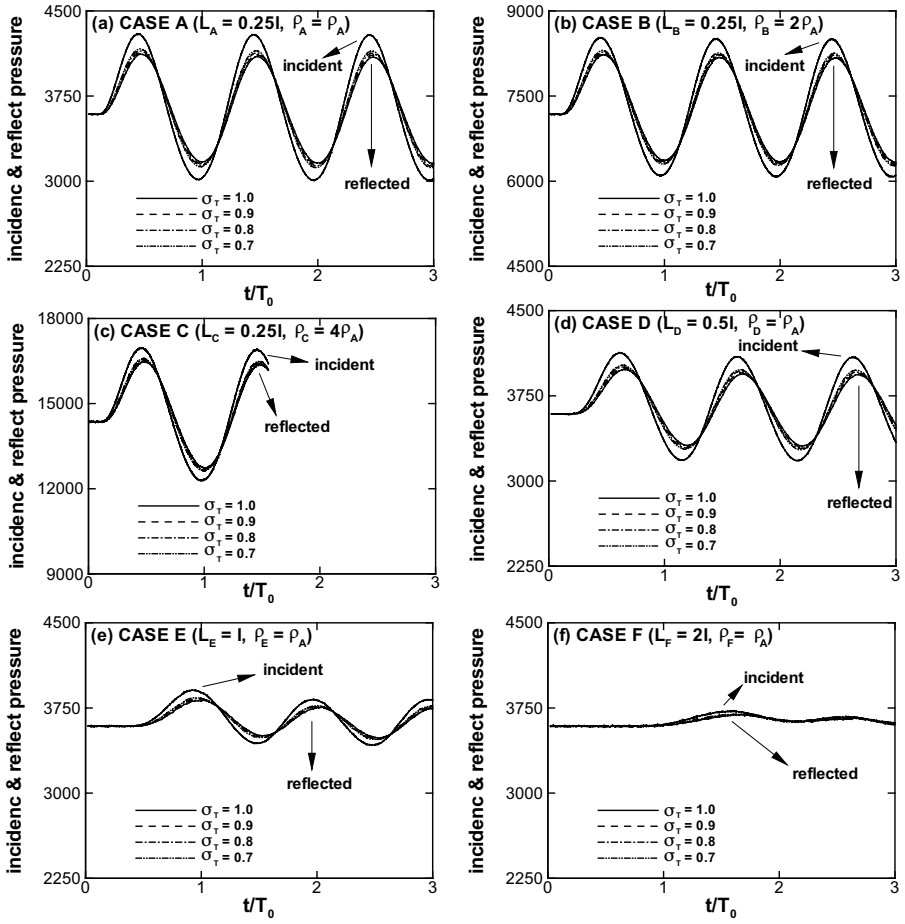

Fig. 7. Temporal variations of incident and reflected wall pressure depending on σ_T for various cases: (a) Case A; (b) Case B; (c) Case C; (d) Case D; (e) Case E; (f) Case F.

Table 3
Averaged positive and negative peak values of heat flux for various cases

Case	Peak value			
	$\sigma_T = 1.0$	$\sigma_T = 0.9$	$\sigma_T = 0.8$	$\sigma_T = 0.7$
A	0.03276 (−0.02572)	0.02946 (−0.02321)	0.02600 (−0.02064)	0.02726 (−0.01794)
B	0.03144 (−0.02523)	0.02846 (−0.02265)	0.02506 (−0.02005)	0.02214 (−0.01739)
C	0.03036 (−0.02580)	0.02734 (−0.02330)	0.02413 (−0.02090)	0.02138 (−0.01837)
D	0.02933 (−0.02456)	0.02705 (−0.02221)	0.02382 (−0.01978)	0.02062 (−0.01694)
E	0.01640 (−0.01420)	0.01470 (−0.01263)	0.01305 (−0.01126)	0.01113 (−0.00965)

different. Also, in either DSMC or free molecular computation, the fundamental errors induced by temperature jump relation also incurred severe discrepancies between direct and indirect results. Rather than the flow properties such as the velocity, temperature and density, the wall heat flux and wall pressure were strongly influenced by the variation of thermal accommodation coefficient because the degree of thermal insulation linearly increased with decreasing thermal accommodation coefficient. However, the difference between indirect and direct heat flux remained unchanged as the thermal accommodation coefficient was varied.

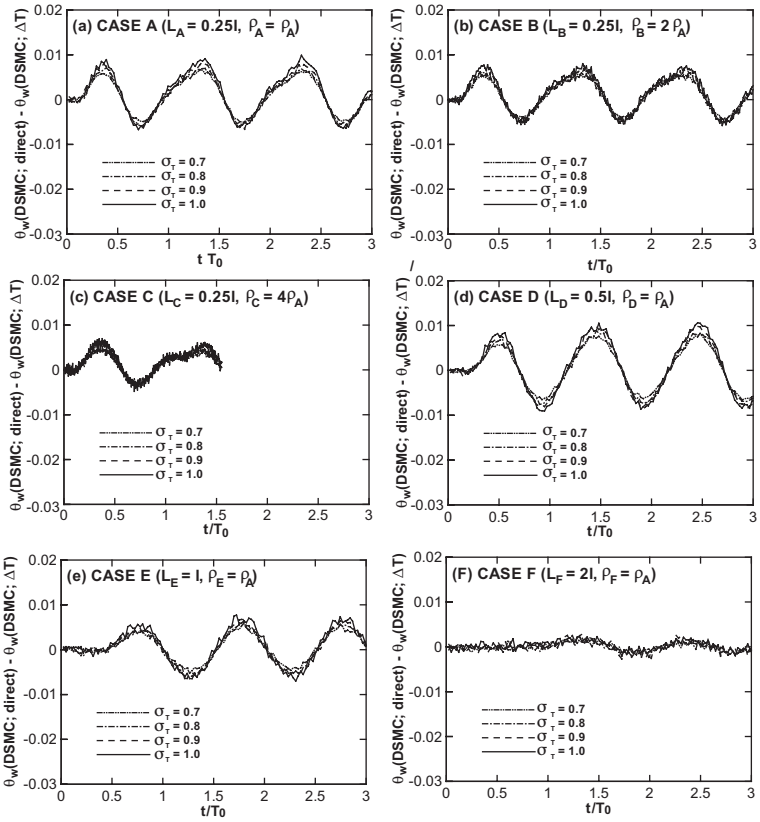

Fig. 8. Temporal variations of θ_w(DSMC; direct) – θ_w(DSMC; ΔT) depending on σ_T for various cases: (a) Case A; (b) Case B; (c) Case C; (d) Case D; (e) Case E; (f) Case F.

Acknowledgement

This work was supported by Korea Research Foundation under Grant (KRF 1999-042-E00021).

References

[1] E.B. Arkilic, M.A. Schmidt, K.S. Breuer, Gaseous slip flow in long microchannels, J. Microelectromech. Syst. 6 (2) (1997) 167–178.
[2] A. Ketsdever, D. Wadworth, E. Muntz, Influence of gas–surface interaction models on predicted performance of a micro-resistojet, AIAA Paper 2000-2430, 2000.
[3] J.H. Park, S.W. Baek, S.J. Kang, M.J. Yu, Analysis of thermal slip in oscillating rarefied flow by using DSMC, Numer. Heat Transfer A 42 (6) (2002) 647–659.
[4] G.A. Bird, Molecular Gas Dynamics and Direct Simulation of Gas Flows, Clarendon Press, Oxford, 1994.
[5] D.T. Lyons, Measuring the thermal accommodation coefficient while aerobraking Magellan, in: J. Harvey, G. Lord (Eds.), Rarefied Gas Dynamics, vol. II, Oxford University Press, Oxford, 1995, pp. 1408–1414.
[6] D.Y. Tzou, Macro- to Microscale Heat Transfer: The Lagging Behavior, Taylor and Francis, New York, 1997.
[7] N.G. Hadjiconstantinou, A.L. Garcia, Molecular simulations of sound wave propagation in simple gases, Phys. Fluids 13 (4) (2001) 1040–1046.
[8] A. Campa, E.G.D. Cohen, Observable fast kinetic eigenmode in binary noble-gas mixtures?, Phys. Rev. Lett. 61 (7) (1988) 853–856.
[9] W. Montfrooij, P. Westerhuijs, V.O. de Haan, I.M. de Schepper, Fast sound in a helium–neon mixture determined by neutron scattering, Phys. Rev. Lett. 63 (5) (1989) 544–546.
[10] J. Fan, I.D. Boyd, C.-P. Cai, K. Hennighausen, G.V. Candler, Computation of rarefied gas flows around a NACA 0012 airfoil, AIAA J. 39 (4) (2001) 618–625.
[11] C.J. Lee, Unique determination of solutions to the Burnett equations, AIAA J. 32 (5) (1994) 985–990.
[12] R.S. Myong, Thermodynamically consistent hydrodynamic computational models for high Knudsen number gas flows, Phys. Fluids 11 (9) (1999) 2788–2802.
[13] J.Y. Yang, J.C. Huang, C.S. Wang, Nonoscillatory schemes for kinetic model equations for gases with internal energy states, AIAA J. 34 (10) (1996) 2071–2081.
[14] Y. Sone, Kinetic theory analysis of linearized Rayleigh problem, J. Phys. Soc. Jpn. 19 (8) (1964) 1463–1473.
[15] Y. Sone, Effect of sudden change of wall temperature in rarefied gas, J. Phys. Soc. Jpn. 20 (2) (1965) 222–229.

[16] W. Huang, D.B. Bogy, The effects of the accommodation coefficient on slider air bearing simulation, J. Tribol. 122 (2000) 427–435.
[17] G.Em. Karniadakis, A. Beskok, Micro-Flows: Fundamentals and Simulation, Springer-Verlag, New York, 2002.
[18] C. Cercignani, M. Lampis, Kinetic models for gas–surface interactions, Transport Theory Stat. Phys. 1 (2) (1971) 101–114.
[19] R.G. Lord, Some extensions to the Cercignani–Lampis gas–surface scattering kernel, Phys. Fluids A 3 (4) (1991) 706–710.
[20] M. Greenspan, Propagation of sound in five monatomic gases, J. Acoust. Soc. Am. 28 (4) (1956) 644–648.
[21] L. Sirovich, J.K. Thurber, Sound propagation according to the kinetic theory of gas, in: J.A. Laurman (Ed.), Rarefied Gas Dynamics, vol. I, Academic Press, New York, 1963, pp. 159–180.
[22] C.H. Chung, S.C Kim, R.M. Stubbs, K.J. De Witt, Low-density nozzle flow by the direct simulation Monte-Carlo and continuum methods, J. Propul. Power 11 (1) (1995) 64–70.